Development of multi-component diesel surrogate fuel models – Part I: Validation of reduced mechanisms of diesel fuel constituents in 0-D kinetic simulations

Poon, Hiew Mun; Pang, Kar Mun; Ng, Hoon Kiat; Gan, Suyin; Schramm, Jesper

Published in:
Fuel

Link to article, DOI:
10.1016/j.fuel.2016.04.043

Publication date:
2016

Document Version
Peer reviewed version

Development of Multi-Component Diesel Surrogate Fuel Models - Part I: Validation of Reduced Mechanisms of Diesel Fuel Constituents in 0-D Kinetic Simulations

Hiew Mun Poon[1], Kar Mun Pang[2], Hoon Kiat Ng[1*], Suyin Gan[3], Jesper Schramm[2]

[1] *Department of Mechanical, Materials and Manufacturing Engineering, The University of Nottingham Malaysia Campus, Jalan Broga, 43500 Semenyih, Selangor, Malaysia.*

[2] *Department of Mechanical Engineering, Danmarks Tekniske Universitet, Nils Koppels Allé, Bygning 403, 2800 Kgs. Lyngby.*

[3] *Department of Chemical and Environmental Engineering, The University of Nottingham Malaysia Campus, Jalan Broga, 43500 Semenyih, Selangor, Malaysia.*

* Corresponding author: Tel: +603 89248161; Fax: +603 89248017; Email-address: hoonkiat.ng@nottingham.edu.my (H.K. Ng)

Abstract

In the present work, development and validation of reduced chemical kinetic mechanisms for several different hydrocarbons are performed. These hydrocarbons are potential representative for practical diesel fuel constituents. n-Hexadecane (HXN), 2,2,4,4,6,8,8-heptamethylnonane (HMN), cyclohexane (CHX) and toluene are selected to represent straight-alkane, branched-alkane, cyclo-alkane and aromatic compounds in the diesel fuel. A five-stage chemical kinetic mechanism reduction scheme formulated in the previous work is applied to develop the reduced HMN and CHX models based on their respective detailed mechanisms. Alongside with the development of the reduced CHX model, a skeletal toluene sub-mechanism is constructed since the elementary reactions for toluene are subset of the detailed CHX mechanism. The final reduced HMN mechanism comprises 89 species with 319 elementary reactions, while the final reduced CHX mechanism which includes the toluene sub-mechanism consists of 80 species with 287 elementary reactions. Both reduced models are approximately 92 % smaller than their respective detailed models in terms of total

number of species and elementary reactions. Following that, both the newly developed fuel constituent reduced mechanisms, together with the formerly derived reduced HXN mechanism are comprehensively validated in zero-dimensional chemical kinetic simulations under a wide range of shock tube and jet-stirred reactor (JSR) conditions. Well agreement between the reduced and detailed mechanisms is achieved for ignition delay (ID) and species concentration predictions under both auto-ignition and JSR conditions, with a maximum relative error of 40 %. In addition, the reduced models are further validated against the JSR experimental results for each diesel fuel constituents. The surrogate models are able to reasonably reproduce the experimental species concentration profiles in view of their simplified fuel chemistries. Deviations within one order of magnitude in the absolute values are recorded between the computations and measurements. Validation of these reduced models for each diesel fuel constituents in this work serves as a prerequisite for constructing a multi-component diesel surrogate fuel model. The compact yet accurate chemical models proposed here aid to reduce the chemistry size of the final multi-component diesel surrogate model such that it remains computationally efficient when it is incorporated with multi-dimensional CFD simulations. The reduced mechanism of each fuel constituent can also be used individually for other CFD applications.

Keywords: mechanism reduction, diesel fuel, branched-alkanes, cyclo-alkanes, aromatics.

1. Introduction

Diesel fuels primarily comprise complex mixtures of different types of hydrocarbon species that can be categorised into several basic structural classes of compounds such as straight-alkanes (also known as n-alkanes), branched-alkanes (also known as iso-alkanes), cyclo-alkanes, and aromatic compounds. For example, typical North American diesel fuels generally consist of 25 % to 50 % of straight- and branched-alkanes, 20 % to 40 % of cyclo-alkanes as well as 15 % to 40 % of aromatic compounds [1].

Among all these classes, straight-alkanes are usually the most abundant components in liquid fuels [2,3]. For the past decades, surrogate models with short carbon chain, such as n-heptane, are generally employed as the representatives for diesel fuels. Nonetheless, it is found that the short-chain surrogate fuel models are inadequate to represent the combustion kinetics of the actual fuels [1,4,5]. Hence, surrogate models for long-chain, straight-alkanes such as n-dodecane, n-tetradecane, and n-hexadecane (HXN) are developed owing to their comparable boiling range to those of the diesel fuels [6]. Hence, these models can potentially be used as diesel fuel surrogate models in multi-dimensional computational fluid dynamics (CFD) modelling studies. In particular, HXN is one of the favourable options as it is the diesel primary reference fuel which permits fuel blending with greater extent of cetane number (CN) range. Of late, there has been considerable progress on the development of chemical kinetic mechanisms for HXN [6–9]. Apart from the kinetic modelling studies, it is noteworthy that HXN has also started to gain popularity in multi-dimensional numerical simulations. For instance, a reduced HXN mechanism with 381 species was successfully derived from the parent mechanism in the study of Liang et al. [10]. The reduced model was subsequently used to simulate homogeneous charge compression ignition (HCCI) combustion of HXN. In addition to that, diesel spray combustion in a constant volume combustion chamber was also simulated by Poon et al. [11] using a compact HXN model. Despite the various reported success of these HXN models, employing HXN alone as a single-component diesel fuel surrogate is not suggested owing to its different hydrogen/carbon molar ratio (H/C) as compared to that of the actual diesel fuels [5,12]. Hence, it is recommended to integrate HXN with other diesel fuel constituents in a surrogate blend to match the diesel fuel kinetics, compositions and CN.

The iso-alkanes are usually lightly branched with only one or two methyl substituents on a long carbon chain [2,3]. To date, iso-octane is the most studied branched-alkane and it has an

76 octane number of 100 [13]. It is a primary reference fuel for gasoline that is difficult to ignite
77 [14]. On the other hand, the highly branched 2,2,4,4,6,8,8-heptamethylnonane (HMN), which
78 is also known as iso-cetane, has been gaining increasing attention as it is a cetane rating
79 reference compound for diesel fuel with CN of 15. This ignition property is important in
80 producing fuel mixtures with different CN when it is integrated with HXN. In view of its
81 importance as a potential surrogate component for the diesel fuels, recent studies have been
82 carried out using HMN with the use of experimental and kinetic modelling approaches [15–
83 18]. A novel chemical kinetic model has been generated by Oehlschlaeger et al. [18] to
84 describe the oxidation of HMN based on the formerly derived iso-octane mechanism [19].
85 The model has successfully captured the ignition delay (ID) behaviour of HMN oxidation
86 under shock-tube conditions, which is also the first ID measurement for HMN thus far.
87 Although multi-dimensional CFD modelling for HMN fuel combustion has yet to be reported
88 in the literature, a reduced model is expected to be useful for the integration with HXN
89 mechanism to produce a compact diesel surrogate fuel model.

90 On the other hand, cyclo-alkanes which consist of a cyclic structure, are an important
91 chemical class of hydrocarbons found in diesel fuels [20,21]. It is noted that the amount of
92 cyclo-alkanes in the fuels might influence the fuel ignition quality as well as soot emission
93 performances [21]. The presence of cyclo-alkane components in the fuels can increase soot
94 production as they generate aromatic compounds through dehydrogenation process, which
95 acts as the inception sites for soot growth [21]. Based on literature, the simplest forms of
96 cyclo-alkanes, namely cyclopentane and cyclohexane (CHX), have received much attention
97 in both experimental investigations and modelling work lately [20–24]. These two
98 components have been widely studied in shock tubes [22,25–27], jet-stirred reactors (JSR)
99 [20,23,28], laminar pre-mixed flames [24,29] and plug flow reactors [30]. According to the
100 modelling study of Ra and Reitz [31], CHX has been chosen as a surrogate to represent the

cyclo-alkane component in the diesel fuels. This representative surrogate is successively applied to formulate a multi-component chemical kinetic model for CFD modelling of HCCI and direct injection engine combustion. Apart from that, more recently, a 50-species reduced chemical kinetic mechanism for CHX has also been successfully incorporated into the multi-dimensional CFD code to model the auto-ignition processes in an rapid compression machine (RCM) under HCCI engine-like conditions [32].

Last but not least, aromatics compounds in diesel fuels are cyclic, planar hydrocarbons with alternating double and single bonds between carbon atoms, forming a continuous ring [2]. Based on the review of Farrell et al. [1], toluene is recommended as the near-term surrogate component for aromatics, by taking into the considerations of the availability of kinetic models and data for all aromatic compounds. Besides, toluene is often integrated into various diesel surrogate fuel blends [33–35] for soot formation modelling as it plays an important role in the formation of polycyclic aromatic hydrocarbons (PAH) and soot precursors. Inclusion of aromatics as a diesel fuel constituent is expected to improve the predictions of soot formation process.

Set against this background, this study aims to develop reduced chemical models which are good representatives for branched-alkanes, cyclo-alkanes and aromatic compounds in typical diesel fuel. The reduced models for each diesel fuel components are then comprehensively validated in zero-dimensional (0-D) chemical kinetic simulations under a wide range of shock tube and JSR conditions. Similar validation exercises are also carried out on the previously derived reduced HXN mechanism which is a surrogate component for straight-alkane in the diesel fuel model.

2. Development of Reduced Chemical Kinetic Mechanisms for Diesel Fuel Constituents

In this work, HXN [6], HMN [18], CHX [21] and toluene [21] are proposed to represent the diesel fuel components. The straight-alkane, HXN, and the branched-alkane, HMN, are diesel primary reference fuels. HMN has a CN of 15 and its combination with HXN provides the capability to vary the CN of the diesel surrogate fuel models. CHX is selected to represent the cycloalkane component in diesel fuel as it is capable of representing the major reaction characteristics of cyclo-alkane oxidation process even though it is the simplest compound [21]. Besides, it may also have a greater effect on soot production as compared to non-cyclic alkane whereby the oxidation routes directly yield aromatic species as intermediates [1]. On the other hand, toluene has one of the simplest molecular structures of the alkylated benzenes and it is regarded as a good representative of the characteristics of aromatic fuels [36].

It is noteworthy that all these fuel constituent models are essentially constructed based on the hierarchical nature of hydrocarbon–oxygen systems [6,18,21] which take into account the kinetics of H_2/CO oxidations as well as small hydrocarbon species which are typically formed in fuel decomposition. These pools of species can then be shared by the fuel constituents in the final multi-component diesel surrogate fuel mechanisms during the model integration [37,38].

2.1 Five-Stage Chemical Kinetic Mechanism Reduction Scheme

The five-stage chemical kinetic mechanism reduction scheme developed in the previous work [11,39] is applied to derive reduced mechanisms for each diesel fuel components. The reduction scheme is illustrated in Fig. A1 in Appendix A. The mechanism reduction scheme consists of five reduction phases such as Directed Relation Graph with Error Propagation (DRGEP) [40,41] using Dijkstra's algorithm [42], isomer lumping [43,44], reaction path analysis, Directed Relation Graph (DRG) [45,46] as well as adjustment of reaction rate constant [37,44,47,48].

During the DRGEP reduction, CO, CO_2, HCO, HO_2, H_2O_2, H_2, and N_2 are chosen as "target species" to determine their shortest pathways to all other species using the Dijkstra's algorithm [42]. A Direct Interaction Coefficient (DIC) is applied to calculate the dependency of a species on another based on its impact to the total production or consumption rate. DIC of species *y* to the production rate of species *x* is expressed by the following equation:

$$\mathrm{DIC} = \frac{\left|\sum_{i=1}^{N_R} v_{x,i}\omega_i\delta_y^i\right|}{\max\left(\underbrace{\sum_{i=1}^{N_R}\max(0, v_{x,i}\omega_i)}_{P_x}, \underbrace{\sum_{i=1}^{N_R}\max(0, -v_{x,i}\omega_i)}_{C_x}\right)} \quad (1)$$

where N_R is the total number of elementary reactions in the mechanism. $v_{x,i}$ is the stoichiometric coefficient of species *x* while ω_i is the net production rate of i^{th} elementary reaction. P_x is the overall production rate of species *x* and C_x is the overall consumption rate of species *x*. δ_{yi} denotes the participation of species *y* in i^{th} elementary reaction and it is defined as:

$$\delta_{yi} = \begin{cases} 1, & \text{if the } i^{th} \text{ elementary reaction involves species } y; \\ 0, & \text{otherwise;} \end{cases} \quad (2)$$

Then, an Overall Interaction Coefficient, R_{xy}, is introduced to determine the maximum of all dependency pathways for all species relative to the targets. It is defined as:

$$R_{xy} = \max_{\text{all path } p}\left(\prod_{j=1}^{N_S-1} r_{s_j s_{j+1}}\right) \quad (3)$$

where *j* refers to the j^{th} species of pathway *p*. *S* is the placeholder for the intermediate species which starts at species *x* and ends at species *y*. N_S is the total number of species in the mechanism. *r* is equivalent to DIC presented in Equation (1). Here, the error tolerance set for the DRGEP reduction is $5\text{x}10^{-4}$. Hence, species with R_{xy} values lower than the user-specified tolerance are eliminated from the mechanism.

Accordingly, species with similar thermodynamic and transport properties are lumped together while insignificant isomers with concentration level lower than $1x10^{-10}$ mole/cm^3 are eliminated.

Following that, main reaction pathways during the fuel oxidation process are analysed using the reaction path analyser of CHEMKIN-PRO software and reactions of species with low normalised temperature *A*-factor sensitivity are removed. The normalised temperature *A*-factor sensitivity is expressed by Equation (4) [49]:

$$\text{Normalised Temperature } A - \text{Factor Sensitivity} = \frac{Individual\ Temperature\ Sensitivity\ Coefficient\ Value}{Total\ Temperature\ Sensitivity\ Coeffcient\ Value} \quad (4)$$

Subsequently, DRG is performed to remove species which have lost pathway connection to the fuel species. Here, the threshold limit is set to unity in order to identify all the coupled species through graph searching using a species coupling measure, r_{xy}. r_{xy} is a normalised contribution of species *y* to the production rate of species *x* and it is expressed as:

$$r_{xy} = \frac{\sum_{i=1,N_R}|v_{x,i}\omega_i\delta_{yi}|}{\sum_{i=1,N_R}|v_{x,i}\omega_i|} \quad (5)$$

Large-scale elimination of species and reactions from the detailed mechanisms commonly causes deviations in the ID and species concentration predictions. Consequently, appropriate optimisation of the reaction rate constants is carefully performed [37,44,47,48]. Further description of the mechanism reduction scheme is detailed in the previous work [11,39].

2.2 Fuel Constituent Base Mechanisms for Kinetic Model Reduction

Here, detailed models of HXN (2,116 species, 8,130 elementary reactions), HMN (1,114 species, 4,469 elementary reactions) and CHX (1,081 species, 4,269 elementary reactions) developed by Westbrook et al. [6], Oehlschlaeger et al. [18] and Silke et al. [21], respectively

are employed as parent mechanisms for kinetic model reduction. The reduced model for HXN comprising 79 species with 289 elementary reactions has been derived in the previous work [11] and thus it is directly applied here. Also, the elementary reactions for toluene are subset of the detailed mechanism of CHX. Both CHX and toluene are important components for benzene production, which acts as a 'connecting species' between them through several reaction pathways. Consequently, the mechanism reduction is carried out for the detailed mechanisms of HMN and CHX in the current study as there is no reported work on the formulation of these mechanisms beforehand.

2.3 Mechanism Reduction Procedures

Similar to the previous mechanism reduction exercise [11], capability of the mechanisms in auto-ignition predictions is selected as the basis for reduction. Both JSR and auto-ignition conditions are then chosen as data source for mechanism reduction, where sampled data points are obtained over a wide range of initial pressure, initial temperature and equivalence ratio (Φ). The conditions applied for mechanism reduction are demonstrated in Table 1. JSR is included in this study as an additional data source for mechanism reduction as it is important in modelling the steady-state extinction process of the combustion process [47]. Closed homogeneous batch reactor and Perfectly-Stirred Reactor (PSR) models of CHEMKIN-PRO software are applied.

As a result, a reduced HMN mechanism comprising 89 species with 319 elementary reactions and a reduced CHX mechanism comprising 80 species with 287 elementary reactions are successfully derived from the integrated mechanism reduction scheme. In this reduction work, appropriate optimisation of the reaction rate constants are carried out such that the influence of the eliminated reactions is incorporated in the Arrhenius rate constants of the retained reactions in order to maintain accuracy of the model predictions [33,37,48]. As such, the relative errors in the ID and fuel concentration predictions induced by the reduction

procedure are minimised as compared to the computations of the detailed models. This reaction rate constant optimisation approach has also been successfully demonstrated in the modelling studies of Wang et al. [37,48] and Golovitchev et al. [33]. The approach had significantly improved their model predictions where the reaction rate constants of H-atom abstraction from the fuel species was included as one of their optimisation targets, as with this study. A perturbation by more than a factor of 30 in the *A*-factor Arrhenius constant was also reported in the study of Wang et al. [37]. The optimised rate constants for important reactions in these reduced mechanisms and the associated targeted functions are detailed in Table 2. The rate constant tuning is carried out for reactions with high normalised temperature *A*-factor sensitivity across all the test conditions, as shown in Fig. A2 in Appendix A. The results are calculated based on the temperature sensitivity coefficient values with initial pressure of 60 bar, initial temperature of 950 K and Φ of 1. Results here are demonstrated to provide a clearer description on the rate constant tuning procedure It is observed that not all of the reactions with high temperature sensitivity coefficient values are selected for rate constant tuning. The procedure is performed according to the targeted functions such as improvement of ID at low temperatures and thus changes in ID at other temperature regimes are undesirable. As a result, reactions with high temperature sensitivity coefficient values which alter IDs at other temperature regimes are not taken into consideration in this case. In order to ensure the IDs at other temperature regimes across all the test conditions are not affected, the 0-D simulations are repeated whenever the rate constant is adjusted. The reaction rate optimisation process is performed in the following steps:

(i) Sensitivity analysis is carried out for each diesel fuel constituent model by applying the test conditions illustrated in Table 1. Reactions with high normalised temperature *A*-

factor sensitivity (> 0.1) are taken into consideration for the subsequent optimisation procedure.

(ii) The *A*-factor Arrhenius constants for reactions that have significant effects on the ID predictions are calibrated. Concurrently, the resulting key species profiles computed by the reduced models are also monitored. Here, optimisation of the reaction rate constants is performed in order to match the results of the detailed models throughout all the shock tube conditions.

(iii) Calibration of the *A*-factor Arrhenius constants is subsequently carried out to reproduce the key species concentrations under JSR conditions. For instance, results obtained from the sensitivity analysis reveal that reactions (R1)-(R2), (R6) and (R11) shown in Table 2 have significant effects on the consumptions of fuel species such as HXN, HMN and $C_6H_5CH_3$ during oxidation process. Hence, the associated *A*-factor values are adjusted to match the fuel concentration predictions of the detailed models.

(iv) Steps (ii) and (iii) are repeated until satisfactory results in ID and species profiles predictions throughout all the test conditions are obtained. The induced error for each prediction is retained to an error tolerance of 40 %, which is reasonable for large-scale mechanism reduction as reported in the literature [44,51–53]. It should be noted that all the calibrations are first performed by modifying the order of magnitude of the *A*-factor value in order to examine its impact on the model predictions. Further optimisation is then carried out by just altering the values within the same order of magnitude to achieve higher accuracy.

The major reaction pathways for each diesel fuel component are illustrated in Fig. A3 in Appendix A. The key reaction pathways of the fuel combustion are obtained from reaction pathway analysis during the mechanism reduction process. As observed in the fuel oxidation

pathways under similar conditions, the oxidation of n-alkanes varies from that of branched-alkanes in terms of the products formation. However, it is observed that the chemical kinetics of fuel oxidations for HXN, HMN and CHX are similar. For instance, H-atom abstractions on the fuel components are prevailing under fuel-lean conditions while thermal decompositions of the fuel components are more dominant under fuel-rich conditions. For stoichiometric conditions, H-atom abstractions are dominant when temperature is low whereas thermal decompositions are more prevalent when temperature is high [7,17,20].

In this section, the reduced models of the fuel constituents are successfully derived using the five-stage chemical kinetic mechanism reduction scheme. The application of the reduction scheme has contributed to at least 92 % reduction in N_S and 93 % reduction in N_R in the reduced mechanisms as compared to the detailed mechanisms for each fuel constituents. Appropriate optimisation of selected reaction rate constants are performed to minimise the influence of eliminated species and reactions associated to the drastic mechanism reduction that has been carried out. Following that, the surrogate models are carried forward to the next section for model validations.

3. Validations of Surrogate Fuel Models in 0-D Chemical Kinetic Simulations

In this section, validations of the reduced surrogate models are performed in 0-D simulations by comparing the ID timing predictions as well as species concentration profiles of important species to those of the detailed mechanisms. The test conditions applied for the mechanism validations in 0-D simulations are described in Table 1.

3.1 Validations against Detailed Models under Auto-Ignition and JSR Conditions

Comparisons of ID timing predictions between the reduced and detailed mechanisms are demonstrated in Fig. 1. Here, only results for the initial pressure of 60 bar are presented. Same pattern is observed for the ID timing plots at initial pressures of 40 bar and 80 bar,

which is characterised by the *S*-shaped curve for ID profiles. It is observed that reasonably good agreements are achieved between the reduced and detailed mechanisms in ID predictions for each diesel fuel constituent. In this reduction work, deviations in ID are relatively evident at low and intermediate temperatures for auto-ignition conditions. Hence, further reduction will deteriorate the ID predictions as reaction pathways are more complex at this temperature range. The current results are considered satisfactory as the induced error for each prediction retains within the error tolerance of 40 % [44,51–53].

In addition, capability of the reduced models for each fuel constituents in replicating concentration of important combustion products is monitored throughout this reduction work. Comparisons of the reduced and detailed mechanisms with respect to species concentration profiles for auto-ignition as well as JSR conditions are shown in Fig. 2 and Fig. 3, respectively. Only results for Φ of 1 are presented since similar temporal evolution trends in the results are obtained for both Φ of 0.5 and 2.

As shown in Fig. 2(a), there is a discrepancy between the computed fuel profiles using the detailed and reduced models of HXN. This may be partly due to the elimination of hexadecyl radical isomers in the reduced model during the reaction path analysis. As a result, the decomposition rate of the fuel species computed by the reduced HXN model is lower than that of the detailed model at the beginning of oxidation process, which eventually leads to the deviation in the temporal evolution trends for HXN. However, the influence of the deviation is not pronounced. The associated IDs as well as the mole fractions of the minor species and products computed by the reduced HXN model are still in good agreement with those of the detailed model. Furthermore, Fig. 2(b) shows that the selected species mole fractions are reasonably replicated for the HMN auto-ignition condition. On the other hand, a consistent distance between the computed species mole fraction using the reduced and detailed CHX models is observed in Fig. 2(c). This is attributed to the shorter ID calculated by the reduced

CHX model as shown earlier in Fig 1(c)(ii). Despite of this, the computed absolute species mole fractions agree with those of the detailed counterpart. Besides, satisfactory results are also obtained in species concentration predictions between the reduced and detailed models for fuel oxidations under the JSR condition, as demonstrated in Fig. 3. The findings here demonstrate an acceptable compromise in terms of mechanism size and results accuracy.

3.2 Validations against JSR Experimental Measurements

Furthermore, the reduced mechanisms for the diesel surrogate fuel components are further validated using the JSR experimental results of HXN, HMN and CHX oxidations carried out by Ristori et al. [7], Dagaut et al. [17] and Voisin et al. [20], respectively. The open PSR model of CHEMKIN-PRO software is employed here to simulate the homogeneous condition of JSR experiments at steady state [54–56]. The validation results are depicted in Fig. 4 by comparing the computed species concentrations to the corresponding experimental measurements for fuel-oxygen mixtures, diluted by nitrogen. The selected species for comparison studies here are reactants (such as HXN, HMN, CHX, O_2), oxygenated products (such as CO_2, CH_2O) as well as important products under fuel-rich region (such as C_2H_2, C_2H_4 and C_6H_6). These species concentrations are validated to ensure that the proposed surrogate models are able to provide a reasonable representation of the kinetics of the fuel oxidations. Apart from that, concentration profiles of C_2H_2, C_2H_4 and C_6H_6 are monitored as they are the major species involved in the soot formation. Both C_6H_6 and C_2H_2 are commonly used as soot precursors while the latter is also the soot surface growth species which is important to soot mass addition during surface growth process. On top of these, C_2H_4 is the most abundant alkene among all the measured alkenes and it plays an important role in the formation of C_2H_2. Thus, validation of concentration profiles of these rich combustion products is expected to aid soot formation predictions for the subsequent multi-dimensional

CFD modelling studies. As soot is mainly formed in fuel-rich condition, Φ of 1.5 is applied in the subsequent validation exercise.

Results in Fig. 4(a) show that the surrogate model for HXN is able to reproduce the species concentration profiles and kinetics of the fuel oxidation adequately in view of its simplified fuel chemistry. It is observed that the computed fuel profile is comparable with the experimental measurement in which the fuel concentration decreases with temperature. However, there is a minor deviation in the fuel concentration predictions as compared to the experimental measurements. The fuel concentration for HXN oxidation at high temperatures (≥ 1000 K) is under-predicted. Owing to the different fuel consumption rate, the formation of product species such as CH_2O also differs from the experimental profiles across the temperature range. An opposite trend is also observed for C_2H_4 and CH_2O profiles between experimental data and those predicted by the reduced models, where the measured concentrations increase with increasing temperatures. This may be expected since the detailed model also predicted an opposite trend for these species, where decreasing trends are observed at high temperature region. The patterns produced by the reduced and detailed models are however consistent. Moreover, as the experimental measurement of C_2H_2 concentration of the HXN oxidation is not available, the computed profile is added in Fig. 4 and is compared to that of the C_2H_4. Based on the reaction path analysis of fuel oxidation routes, the formation of C_2H_2 is significantly dependent on C_2H_4. It is observed that both C_2H_4 and C_2H_2 concentrations increase with temperature when T < 1100 K. However, C_2H_4 concentration starts to decrease thereafter while C_2H_2 concentration continues to rise. This could be attributed to the consumption of C_2H_4 which leads to the formation of C_2H_2 [57]. In addition, the species concentration profiles predicted by the reduced mechanism are also compared with those of the detailed mechanism. Consistency in species profile trends is

observed between the computed results using the reduced and detailed mechanisms, as demonstrated in Fig. 4(a).

Similar to the HXN oxidation, Fig. 4(b) demonstrates that the HMN concentration decreases when ambient temperature increases. Besides, it is also observed that the computed fuel concentration using the reduced chemistry is over-predicted at 800 K < T < 1000 K as compared to the experimental measurements. The deviations between the computed results and the experimental measurements are within one order of magnitude in the absolute values. In spite of this, the species profiles for the resulting product species such as C_2H_2, C_2H_4 and C_2H_6 are seen to be consistent and identical. Additionally, similar temporal evolution trends are observed between the reduced and detailed mechanisms.

Furthermore, based on the results obtained for CHX oxidation in Fig. 4(c), decreasing trend in fuel profile is obtained and fuel concentrations at T > 850 K are under-predicted. Overall agreement is achieved between the species concentration predictions and the experimental measurements. Besides these, the species profile trends predicted by the reduced mechanism are consistent with those of the detailed mechanism.

Although variation of the computed concentrations could reach as high as one order of magnitude as compared to the JSR experimental measurements, the results of the predicted species concentrations are deemed acceptable in view of their simplified fuel chemistries. The overall agreements between the experimental and predicted species profiles for HXN, HMN and CHX are achieved and these fuel constituent models are henceforth used in Part II to construct multi-component diesel surrogate models.

4. Conclusions

In this study, reduced models of branched- (HMN) and cyclo- (CHX) alkanes are developed using the five-stage chemical kinetic mechanism reduction scheme [39,11] formulated in the previous work. With the implementation of the reduction scheme, reductions of 92 % and 93 % in terms of N_S and N_R, respectively, are achieved in comparison to the detailed mechanisms for both fuel constituents. As a result, a reduced HMN mechanism with 89 species and a reduced CHX mechanism with 80 species are developed. Subsequently, both the aforementioned constituent mechanisms, together with the reduced HXN mechanism derived in the previous work are comprehensively validated in 0-D chemical kinetic simulations under a wide range of shock tube and JSR conditions in terms of ID timing and species concentration predictions. The overall ID timings and species concentrations at the test conditions agree well with those calculated using the respective detailed mechanisms. The maximum deviations from the detailed models in ID timing predictions are maintained to within 40 %. Apart from that, trends of the species concentration profiles computed by the fuel constituent reduced models are also retained as compared to those of the detailed models for both auto-ignition and JSR conditions. The relative errors between the computations of the reduced and detailed models remain 40 % throughout the test conditions. In addition, the fidelity of the reduced models is further assessed using the experimental data of respective fuel oxidations in a JSR. The experimental species concentration profiles for each fuel constituents are adequately reproduced with maximum deviations of one order of magnitude in the absolute values.

The construction of the reduced models for each diesel fuel constituents in this work is an essential prerequisite for the developmental work of multi-component diesel surrogate fuel models presented in Part II. These diesel fuel constituent surrogate models are also ready to be used independently for other CFD applications such as HCCI and direct injection engine combustion simulations [10,31]. It is worth mentioning that, the reduced models are

constructed specifically for engine-like operating conditions such that the chemistry can be minimised and a practical level of computational efficiency in multi-dimensional CFD simulations can be achieved. Hence, these mechanisms have to be used with care when they are applied for other applications.

Acknowledgements

The Ministry of Higher Education Malaysia is acknowledged for the financial support towards this project under the Fundamental Research Grant Scheme (FRGS) F0014.54.02. The work at Technical University of Denmark is supported by Innovation Fund Denmark and MAN Diesel & Turbo A/S through the RADIADE project.

References

[1] Farrell JT, Cernansky NP, Dryer FL, Law CK, Friend DG, Hergart CA, et al. Development of an Experimental Database and Kinetic Models for Surrogate Diesel Fuels. SAE Technical Paper 2007-01-0201; 2007.

[2] Morrison RD, Murphy BL. Environmental Forensics: Contaminant Specific Guide. Elsevier; 2005.

[3] Roberts JD, Caserio MC. Basic Principles of Organic Chemistry. WA Benjamin, Inc.; 1977.

[4] Lu T, Law CK. Toward Accommodating Realistic Fuel Chemistry in Large-Scale Computations. Prog Energy Combust Sci 2009;35:192–215.

[5] Meijer M. Characterization of n-Heptane as a Single Component Diesel Surrogate Fuel. Technical University of Eindhoven Automotive Technology, Graduation Thesis; 2010.

[6] Westbrook CK, Pitz WJ, Herbinet O, Curran HJ, Silke EJ. A Comprehensive Detailed Chemical Kinetic Reaction Mechanism for Combustion of n-Alkane Hydrocarbons from n-Octane to n-Hexadecane. Combust Flame 2009;156:181–99.

[7] Ristori A, Dagaut P, Cathonnet M. The Oxidation of n-Hexadecane: Experimental and Detailed Kinetic Modeling. Combust Flame 2001;125:1128–37.

[8] Chaos M, Kazakov A, Dryer FL, Zhao Z, Zeppieri SP. High Temperature Compact Mechanism Development for Large Alkanes: n-Hexadecane. In: 6th Int. Conf. Chem. Kinet., 2005.

[9] Fournet R, Battin-Leclerc F, Glaude PA, Judenherc B, Warth V, Come GM, et al. The Gas-Phase Oxidation of n-Hexadecane. Int J Chem Kinet 2001;33:574–86.

[10] Liang L, Puduppakkam K, Meeks E. Towards Using Realistic Chemical Kinetics in Multidimensional CFD. In: 19th Int. Multidimens. Engine Model. User's Gr. Meet., 2009.

[11] Poon HM, Ng HK, Gan S, Pang KM, Schramm J. Development and Validation of Chemical Kinetic Mechanism Reduction Scheme for Large-Scale Mechanisms. SAE Int J Fuels Lubr 2014;7:653–62.

[12] Galle J, Sebastian V. Influence of Diesel Surrogates on the Behavior of Simplified Spray Models. Proc FISITA 2012 World Automot Congr 2013;189:361–74.
[13] Pitz WJ, Cernansky NP, Dryer FL, Egolfopoulos FN, Farrell JT, Friend DG, et al. Development of an Experimental Database and Chemical Kinetic Models for Surrogate Gasoline Fuels. SAE Technical Paper 2007-01-0175; 2007.
[14] Westbrook CK, Pitz WJ, Mehl M, Curran HJ. Detailed Chemical Kinetic Reaction Mechanisms for Primary Reference Fuels for Diesel Cetane Number and Spark-Ignition Octane Number. Proc Combust Inst 2011;33:185–92.
[15] Agosta A, Cernansky NP, Miller DL, Faravelli T, Ranzi E. Reference Components of Jet Fuels: Kinetic Modeling and Experimental Results. Exp Therm Fluid Sci 2004;28:701–8.
[16] Lenhert DB, Cernansky NP, Miller DL. The Oxidation of Large Molecular Weight Hydrocarbons in a Pressurized Flow Reactor. In: 4th Jt. Meet. US Sect. Combust. Inst., 2005.
[17] Dagaut P, Hadj-Ali K. Chemical Kinetic Study of the Oxidation of Isocetane (2, 2, 4, 4, 6, 8, 8-Heptamethylnonane) in a Jet-Stirred Reactor: Experimental and Modeling. Energy & Fuels 2009;19:2389–95.
[18] Oehlschlaeger MA, Steinberg J, Westbrook CK, Pitz WJ. The Autoignition of iso-Cetane at High to Moderate Temperatures and Elevated Pressures: Shock Tube Experiments and Kinetic Modeling. Combust Flame 2009;156:2165–72.
[19] Curran HJ, Gaffuri P, Pitz WJ, Westbrook CK. A Comprehensive Modeling Study of iso-Octane Oxidation. Combust Flame 2002;129:253–80.
[20] Voisin D, Marchal A, Reuillon M, Boettner JC, Cathonnet M. Experimental and Kinetic Modeling Study of Cyclohexane Oxidation in a JSR at High Pressure. Combust Sci Technol 1998;138:137–58.
[21] Silke EJ, Pitz WJ, Westbrook CK, Ribaucour M. Detailed Chemical Kinetic Modeling of Cyclohexane Oxidation. J Phys Chem A 2007;111:3761–75.
[22] Daley SM, Berkowitz AM, Oehlschlaeger MA. A Shock Tube Study of Cyclopentane and Cyclohexane Ignition at Elevated Pressures. Int J Chem Kinet 2008;40:624–34.
[23] El Bakali A, Braun-Unkhoff M, Dagaut P, Frank P, Cathonnet M. Detailed Kinetic Reaction Mechanism for Cyclohexane Oxidation at Pressure Up to Ten Atmospheres. Proc Combust Inst 2000;28:1631–8.
[24] Law ME, Westmoreland PR, Cool TA, Wang J, Hansen N, Taatjes CA, et al. Benzene Precursors and Formation Routes in a Stoichiometric Cyclohexane Flame. Proc Combust Inst 2007;31 I:565–73.
[25] Tsang W. Thermal Decomposition of Cyclopentane and Related Compounds. Int J Chem Kinet 1978;10:599–617.
[26] Tsang W. Thermal Stability of Cyclohexane and 1-Hexene. Int J Chem Kinet 1978;10:1119–38.
[27] Sirjean B, Buda F, Hakka H, Glaude PA, Fournet R, Warth V, et al. The Autoignition of Cyclopentane and Cyclohexane in a Shock Tube. Proc Combust Inst 2007;31 I:277–84.
[28] Simon V, Simon Y, Scacchi G, Baronnet F. Étude Expérimentale et Modélisation des Réactions d'Oxydation du n-Pentane et du Cyclopentane. Can J Chem 1997;75:575–84.
[29] Davis SG, Law CK. Determination of and Fuel Structure Effects on Laminar Flame Speeds of C1 to C8 Hydrocarbons. Combust Sci Technol 1998;140:427–49.
[30] Billaud F, Chaverot P, Berthelin M, Freund E. Thermal Decomposition of Cyclohexane at Approximately 810 Degree C. Ind Eng Chem Res 1988;27:759–64.
[31] Ra Y, Reitz RD. A Combustion Model for IC Engine Combustion Simulations with

Multi-Component Fuels. Combust Flame 2011;158:69–90.
[32] Griffiths JF, Piazzesi R, Sazhina EM, Sazhin SS, Glaude PA, Heikal MR. CFD Modelling of Cyclohexane Auto-Ignition in an RCM. Fuel 2012;96:192–203.
[33] Golovitchev VI, Bergman M, Montorsi L. CFD Modeling of Diesel Oil and DME Performance in a Two-Stroke Free Piston Engine. Combust Sci Technol 2007;179:417–36.
[34] Wang H, Jiao Q, Yao M, Yang B, Qiu L, Reitz RD. Development of an n-Heptane/Toluene/Polyaromatic Hydrocarbon Mechanism and its Application for Combustion and Soot Prediction. Int J Engine Res 2013;14:434–51.
[35] Ranzi E, Frassoldati A, Stagni A, Pelucchi M, Cuoci A, Faravelli T. Reduced Kinetic Schemes of Complex Reaction Systems: Fossil and Biomass-Derived Transportation Fuels. Int J Chem Kinet 2014;46:512–42.
[36] Pitz WJ, Seiser R, J. W. Bozzelli, K. Seshadri, Chen CJ, Costa ID, et al. Chemical Kinetic Study of Toluene Oxidation Under Premixed and Nonpremixed Conditions. Lawrence Livermore Natl Lab 2003:1–20.
[37] Wang H, Yao M, Reitz RD. Development of a Reduced Primary Reference Fuel Mechanism for Internal Combustion Engine Combustion Simulations. Energy & Fuels 2013;27:7843–53.
[38] Chang Y, Jia M, Li Y, Liu Y, Xie M, Wang H, et al. Development of a Skeletal Mechanism for Diesel Surrogate Fuel by Using a Decoupling Methodology. Combust Flame 2015;162:3785–802.
[39] Poon HM, Ng HK, Gan S, Pang KM, Schramm J. Evaluation and Development of Chemical Kinetic Mechanism Reduction Scheme for Biodiesel and Diesel Fuel Surrogates. SAE Int J Fuels Lubr 2013;6:729–44.
[40] Lu T, Law CK. On the Applicability of Directed Relation Graphs to the Reduction of Reaction Mechanisms. Combust Flame 2006;146:472–83.
[41] Pepiot P, Pitsch H. Systematic Reduction of Large Chemical Mechanisms. In: 4th Jt. Meet. U.S. Sect. Combust. Inst., 2005, p. 1–6.
[42] Dijkstra EW. A Note on Two Problems in Connexion with Graphs. Numer Math 1959:269–71.
[43] Lu T, Law CK. Strategies for Mechanism Reduction for Large Hydrocarbons: n-Heptane. Combust Flame 2008;154:153–63.
[44] Brakora JL, Ra Y, Reitz RD. Combustion Model for biodiesel-Fueled Engine Simulations Using Realistic Chemistry and Physical Properties. SAE Int J Engines 2011;4:931–47.
[45] Lu T, Law CK. A Directed Relation Graph Method for Mechanism Reduction. Proc Combust Inst 2005;30:1333–41.
[46] Lu T, Law CK. Linear Time Reduction of Large Kinetic Mechanisms with Directed Relation Graph: n-Heptane and iso-Octane. Combust Flame 2006;144:24–36.
[47] Cheng X, Ng HK, Gan S, Ho JH, Pang KM. Development and Validation of a Generic Reduced Chemical Kinetic Mechanism for CFD Spray Combustion Modelling of Biodiesel Fuels. Combust Flame 2015;162:2354–70.
[48] Wang H, Yao M, Yue Z, Jia M, Reitz RD. A Reduced Toluene Reference Fuel Chemical Kinetic Mechanism for Combustion and Polycyclic-Aromatic Hydrocarbon Predictions. Combust Flame 2015;162:2390–404.
[49] Pang KM, Ng HK, Gan S. Development of an Integrated Reduced Fuel Oxidation and Soot Precursor Formation Mechanism for CFD Simulations of Diesel Combustion. Fuel 2011;90:2902–14.
[50] Le MK, Kook S. Injection Pressure Effects on the Flame Development in a Light-Duty Optical Diesel Engine. SAE Int J Engines 2015;8:609–24.

[51] Niemeyer KE, Sung C-J, Raju MP. Skeletal Mechanism Generation for Surrogate Fuels Using Directed Relation Graph with Error Propagation and Sensitivity Analysis. Combust Flame 2010;157:1760–70.
[52] Yang J, Johansson M, Naik C, Puduppakkam K, Golovitchev V, Meeks E. 3D CFD Modeling of a Biodiesel-Fueled Diesel Engine Based on a Detailed Chemical Mechanism. SAE Technical Paper 2012-01-0151; 2012.
[53] Luo Z, Plomer M, Lu T, Som S, Longman DE, Sarathy SM, et al. A Reduced Mechanism for Biodiesel Surrogates for Compression Ignition Engine Applications. Fuel 2012;99:143–53.
[54] Battin-Leclerc F, Simmie JM, Blurock E. Cleaner Combustion: Developing Detailed Chemical Kinetic Models. Springer Science & Business Media; 2013.
[56] Dagaut P, Cathonnet M, Rouan JP, Foulatier R, Quilgars A, Boettner JC, et al. A Jet-Stirred Reactor for Kinetic Studies of Homogeneous Gas-Phase Reactions at Pressures Up to Ten Atmospheres (≈1 MPa). J Phys E: Scientific Instruments 1986;19:207–9.
[57] Veloo PS, Dagaut P, Togbé C, Dayma G, Sarathy SM, Westbrook CK, et al. Experimental and Modeling Study of the Oxidation of n- and iso-Butanal. Combust Flame 2013;160:1609–26.

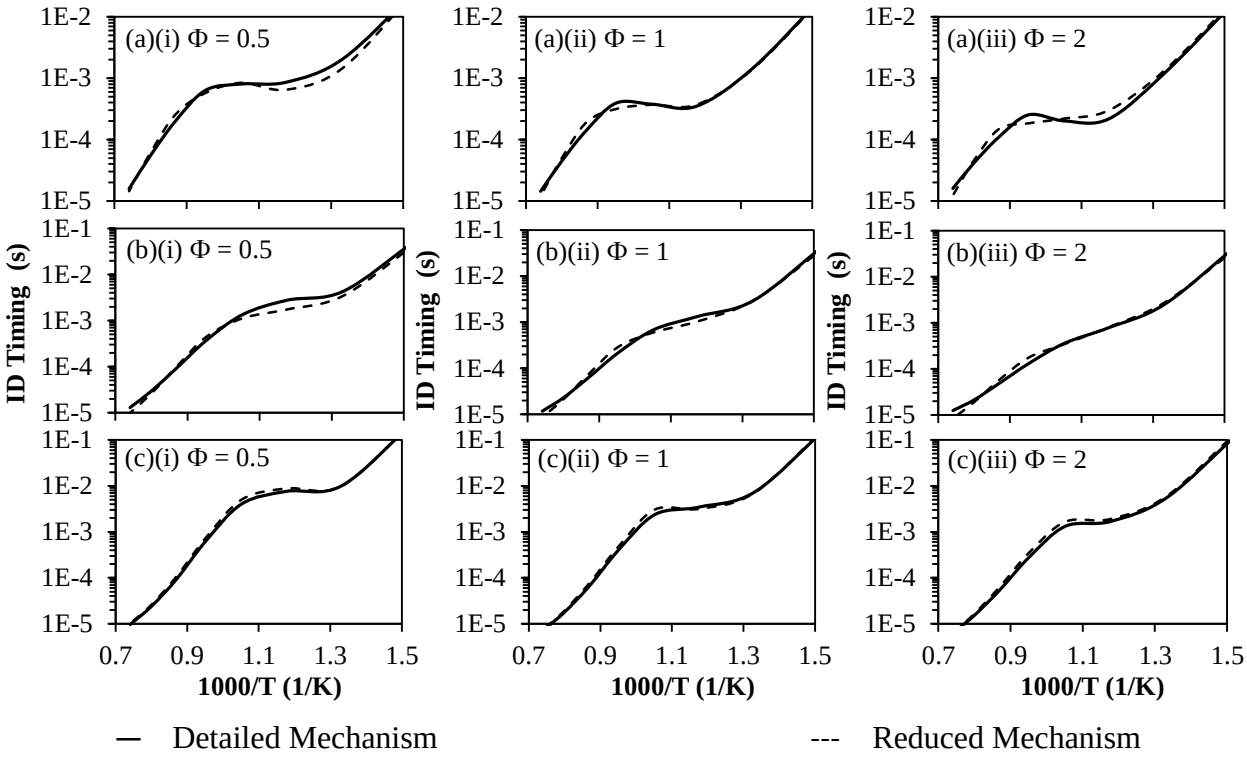

Fig. 1 Computed ID of (a) HXN, (b) HMN and (c) CHX calculated by respective detailed and reduced mechanisms, with initial pressure of 60 bar and Φ of (i) 0.5, (ii) 1.0, (iii) 2.0.

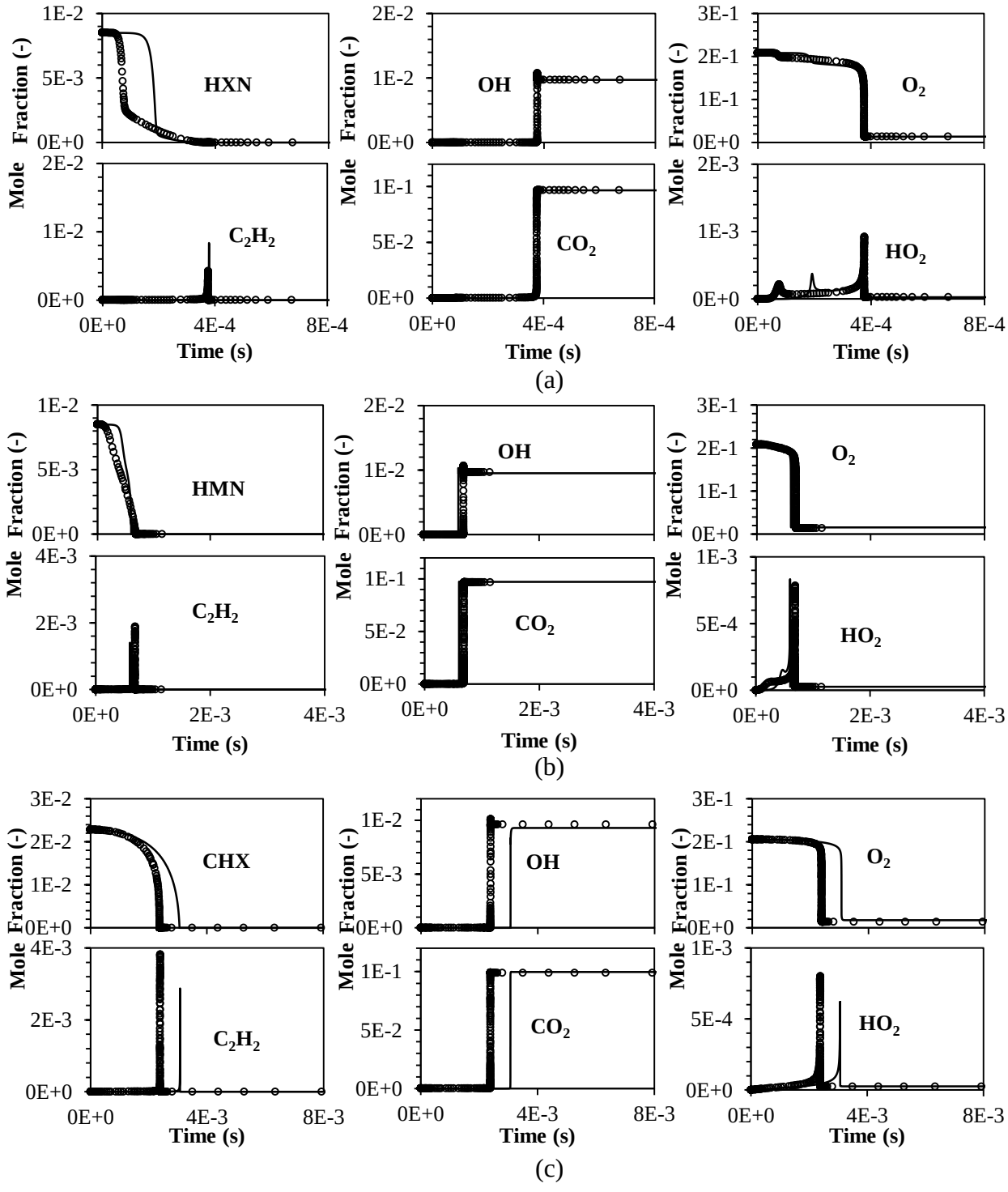

Fig. 2 Computed species profiles for (a) HXN, (b) HMN and (c) CHX combustions under auto-ignition condition, with initial pressure of 60 bar, initial temperature of 950 K and Φ of 1.

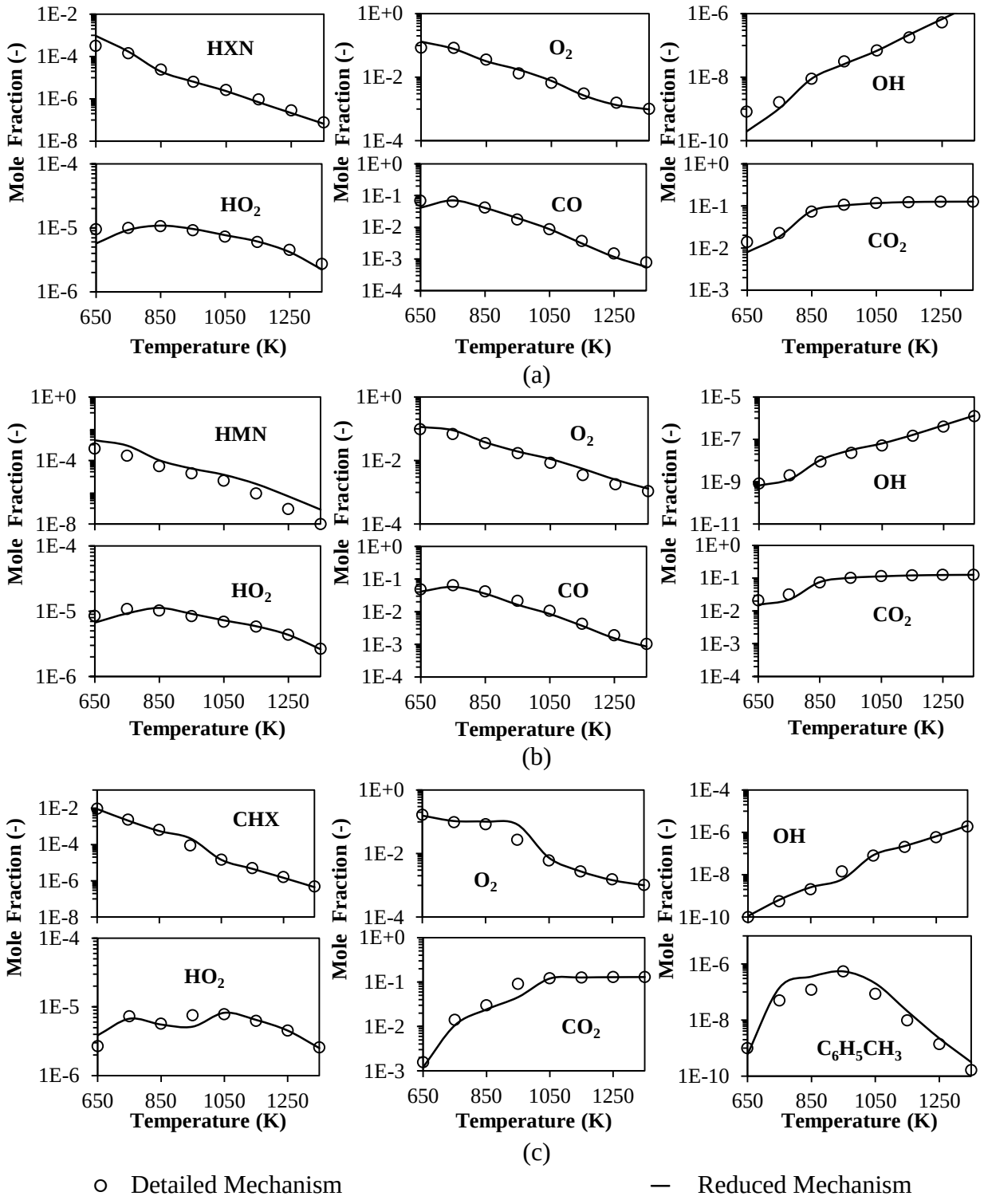

Fig. 3 Computed species profiles of (a) HXN, (b) HMN and (c) CHX oxidations under JSR condition as a function of temperature, with initial pressure of 60 bar and Φ of 1.0.

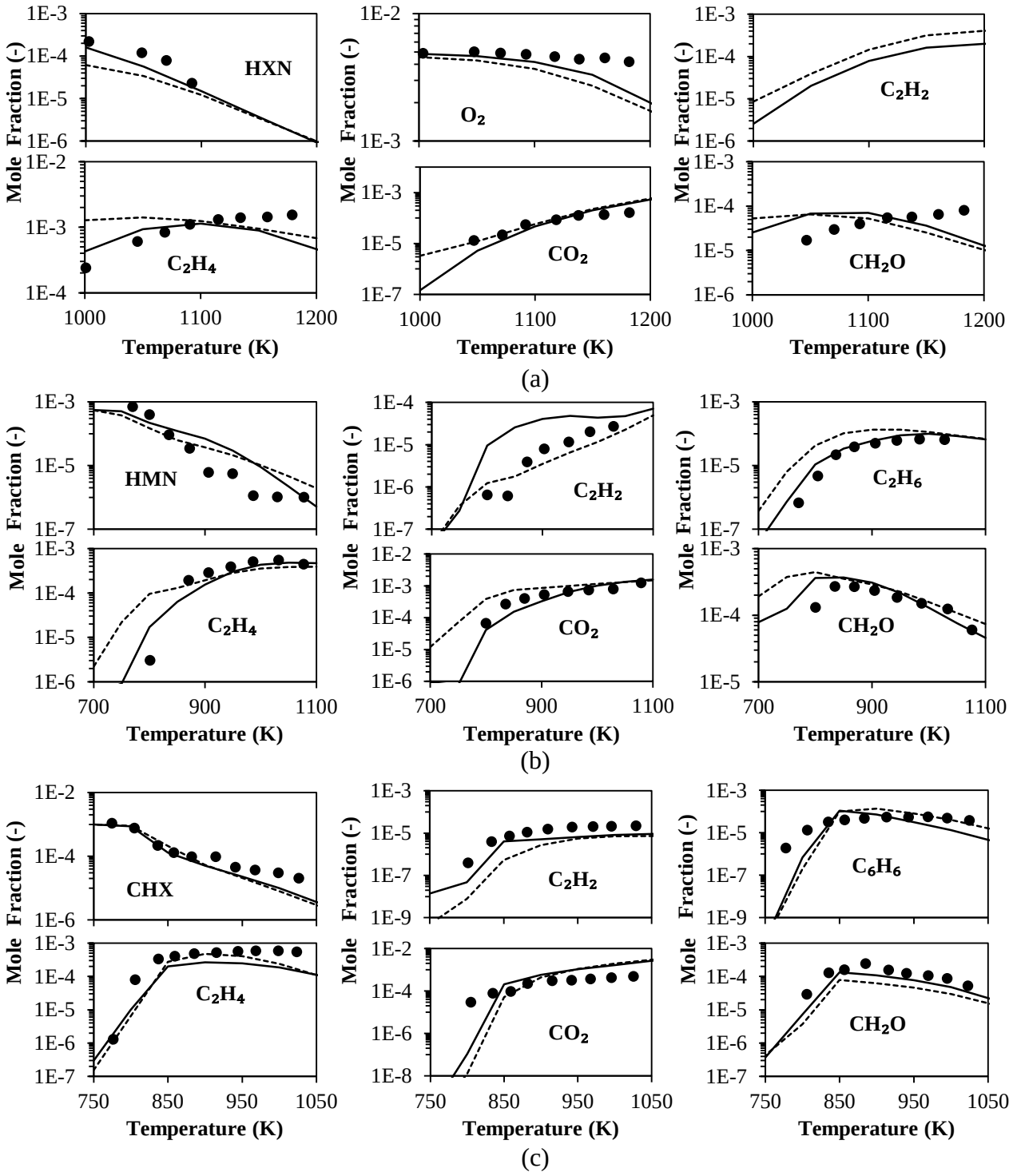

Fig. 4 Computed and experimental species mole fractions obtained from the oxidation of (a) 0.03 % HXN (pressure = 1 atm, Φ = 1.5, residence time = 70 ms), (b) 0.07 % HMN (pressure = 10 atm, Φ = 2, residence time of 1 s), and (c) 0.1 % CHX (pressure = 10 atm, Φ = 1.5, residence time = 0.5 s) in a JSR.

Table 1 Test conditions applied for mechanism reduction as well as validations of the diesel surrogate models.

Operating Conditions		Range Evaluated
Auto-ignition[a]	Equivalence Ratio, Φ (-)	0.5, 1.0, 2.0
	Initial Pressure (bar)	40, 60, 80
	Initial Temperature (K)	650 – 1350 (100 K increments)
JSR[a]	Equivalence Ratio, Φ (-)	0.5, 1.0, 2.0
	Initial Pressure (bar)	40, 60, 80
	Residence Time[c] (s)	1
JSR[b]	Equivalence Ratio, Φ (-)	1.5 (HXN, CHX); 2 (HMN)
	Initial Pressure (bar)	1.01 (HXN); 10.1 (HMN, CHX)
	Residence Time (s)	0.07 (HXN); 1 (HMN); 0.5 (CHX)

[a] Selected operating conditions for mechanism reduction and model validations based on the typical in-cylinder pressure values during the main fuel injection event for light-duty [50], direct-injection diesel engines.

[b] Selected operating conditions for model validations based on the experimental results of HXN [7], HMN [17] and CHX [20] oxidations in a JSR. The unit for pressure is converted from atm to bar (1 atm = 1.01 bar).

[c] Selected residence time based on minimum extinction time at steady-state for combustion at low-, intermediate- and high-temperatures [47].

Table 2 Comparisons of the original and adjusted *A*-factor values of Arrhenius parameters in conjunction with their respective targeted functions for the diesel fuel components.

Reactions	*A*-factor values		Targeted Functions
	Original	Adjusted	
HXN			
(R1) HXN + OH = C16H33-5 + H2O	9.400E07	6.400E08	Improved fuel concentration prediction
(R2) HXN + HO2 = C16H33-5 + H2O2	1.120E13	5.120E14	Improved fuel concentration prediction
(R3) C6H12-1+C10H21-1=C16H33-5	1.000E11	1.000E12	Improved ID prediction at NTC[b]
(R4) C16KET5-7 = OH + NC4H9COCH2 + NC9H19CHO	1.050E16	4.050E16	Improved ID prediction at NTC[b]
HMN			
(R5) TC4H9 + FC12H25 = HMN	8.000E12	4.000E12	Improved ID prediction at high temperature[c]
(R6) HMN + H = HMN-R8 + H2	7.340E05	7.340E06	Improved fuel concentration prediction
(R7) IC4H8 + FC12H25 = HMN-R8	1.000E10	5.000E09	Improved ID prediction at NTC[b]
(R8) HMN-R8O2 = HMN-R8 + O2	3.465E20	7.465E19	Improved ID prediction at NTC[b]
(R9) HMNOOH8-5O2 = HMNOOH8-5 + O2	4.734E27	4.734E26	Improved ID prediction at low temperature[a]
(R10) HMNOOH8-5O2 = HMNKET8-5 + OH	3.125E09	2.125E10	Improved ID prediction at low temperature[a]
CHX			
(R11) C6H5CH3 + OH = C6H5CH2J + H2O	5.190E09	5.190E07	Improved concentration prediction of toluene
(R12) CHXO2J = CHX1Q3J	1.860E11	2.860E11	Improved ID prediction at low temperature[a]

[a]Low-temperature region: 650 – 850 K

[b]NTC region: 850 – 1050 K

[c]High-temperature region: 1050 – 1350 K

Appendix A: Chemical Kinetic Mechanism Reduction

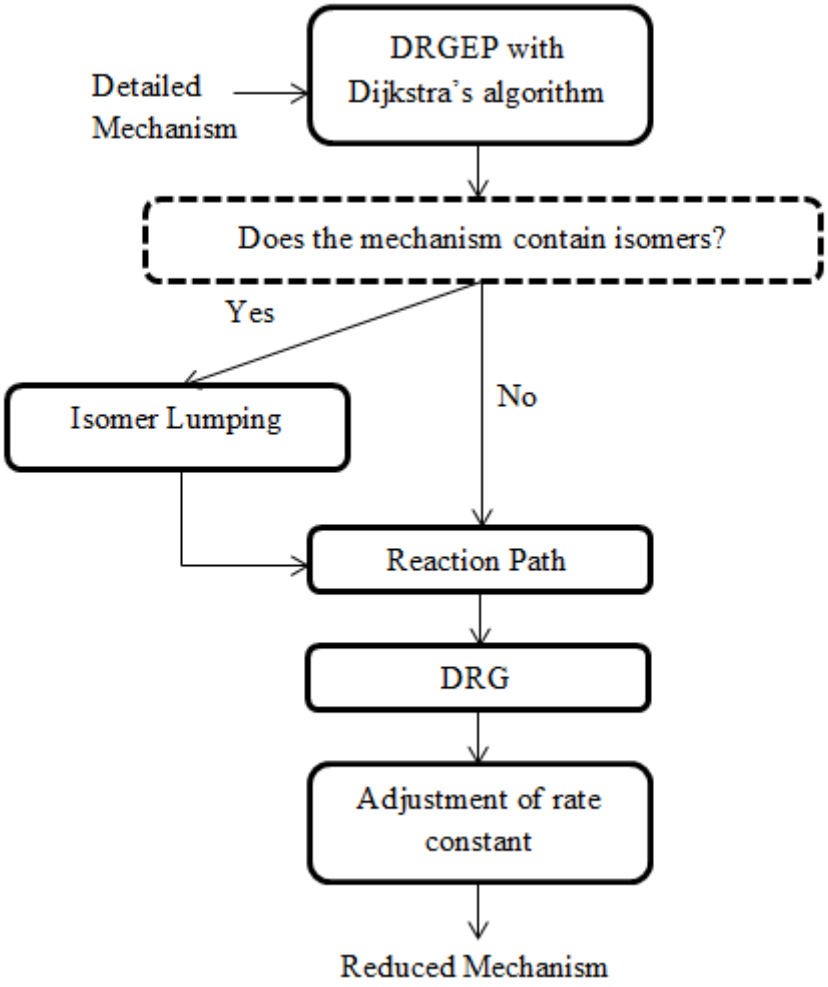

Fig. A1 Flow chart of the five-stage chemical kinetic mechanism reduction scheme [11,37].

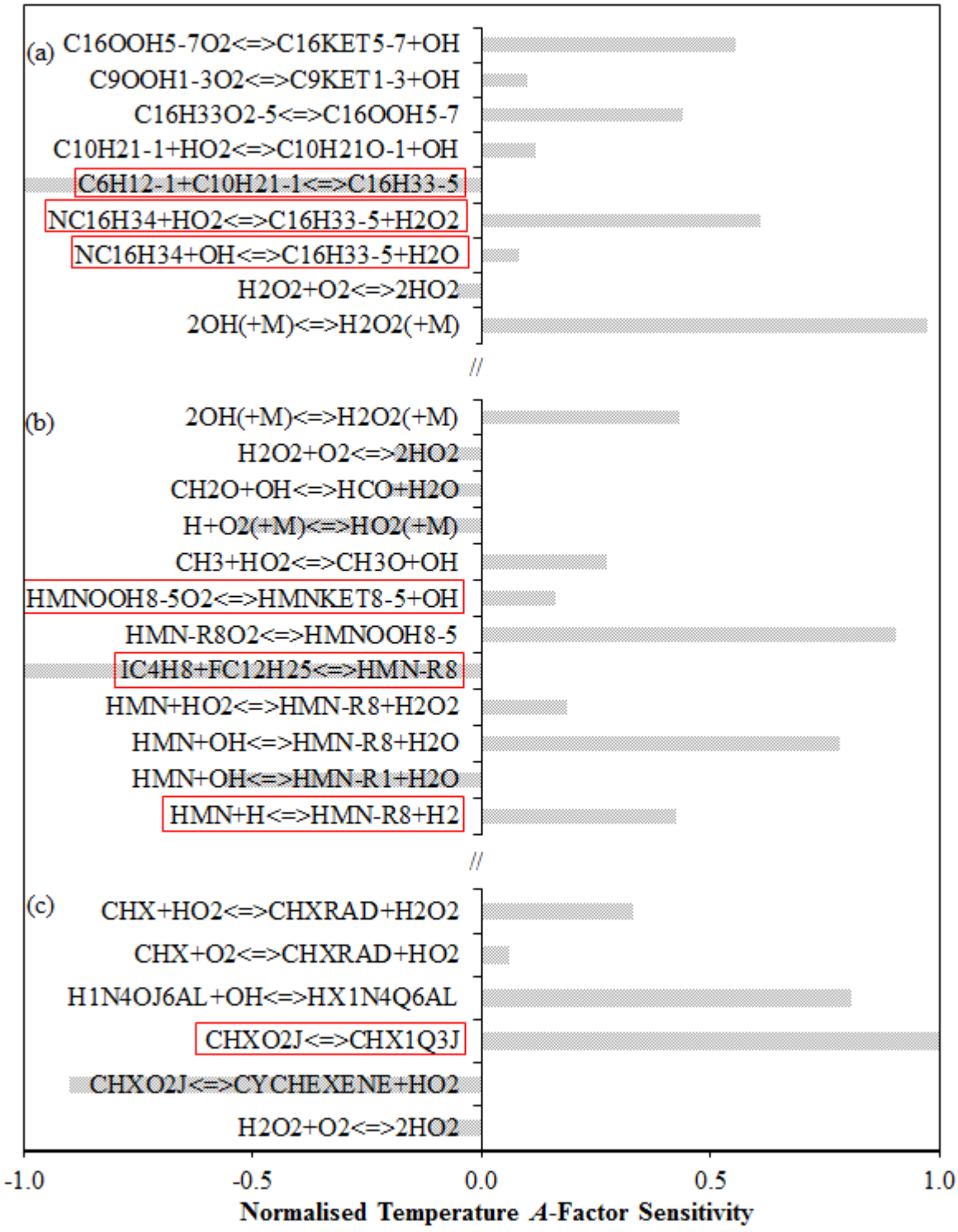

Fig. A2 Reactions with normalised temperature *A*-factor sensitivities for reduced mechanisms of (a) HXN, (b) HMN and (c) CHX, with initial pressure of 60 bar, initial temperature of 950 K and Φ of 1. [Note: Red boxes indicate the reactions selected for adjustment of the *A*-factor values of Arrhenius parameters.]

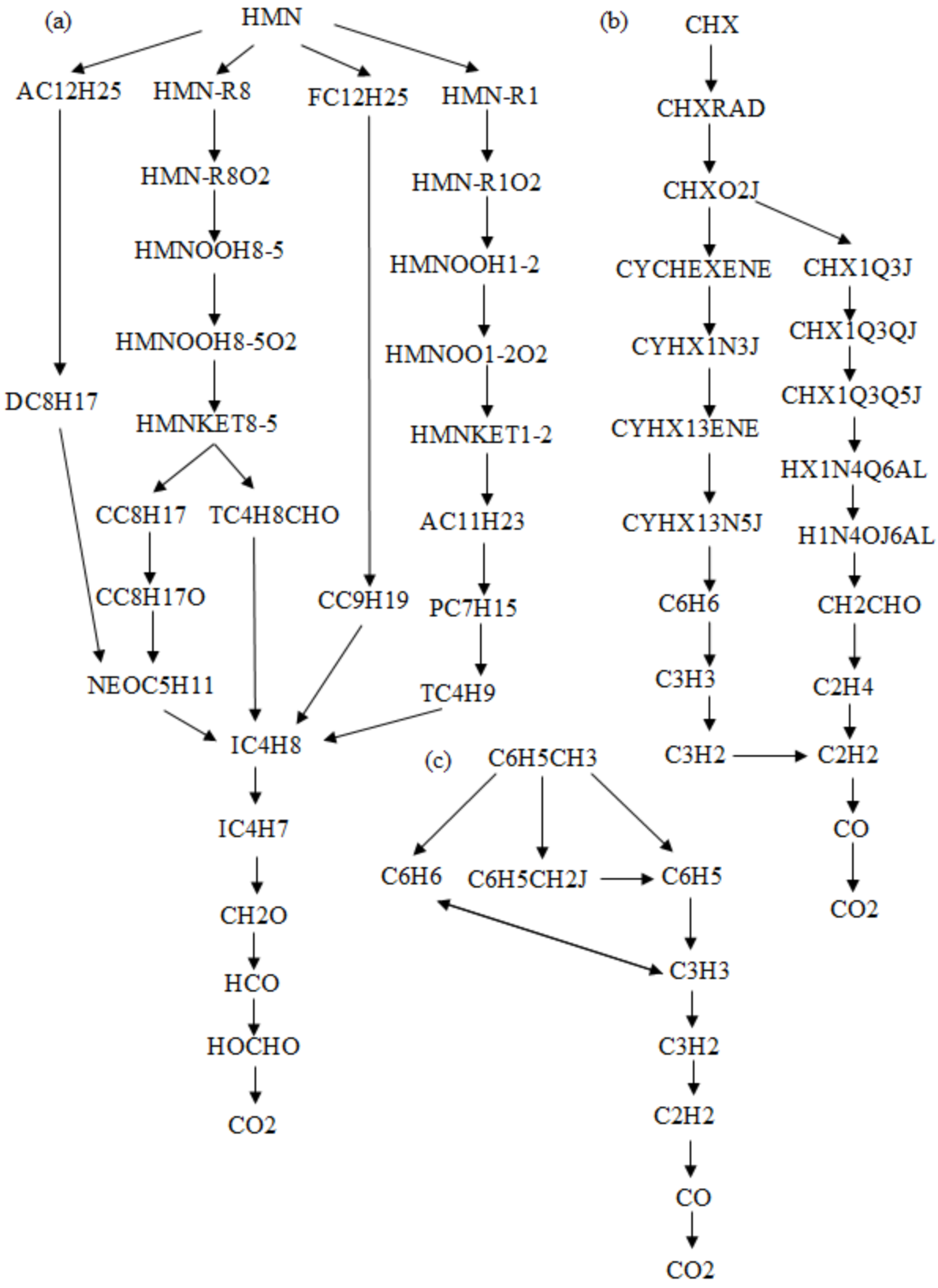

Fig. A3 Main reaction pathways of (a) HMN, (b) CHX and (c) toluene ($C_6H_5CH_3$) during fuel oxidation process for an initial pressure of 60 bar, initial temperature of 950 K and Φ of 1.